THE RABIT: A RAPID AUTOMATED BIODOSIMETRY TOOL FOR RADIOLOGICAL TRIAGE

Guy Garty,* Youhua Chen,[†] Alessio Salerno,[†‡] Helen Turner,* Jian Zhang,[†]
Oleksandra Lyulko,* Antonella Bertucci,* Yanping Xu,* Hongliang Wang,[†]
Nabil Simaan,[†] Gerhard Randers-Pehrson,* Y. Lawrence Yao,[†] Sally A. Amundson,*
and David J. Brenner*

Abstract—In response to the recognized need for high through-put biodosimetry methods for use after large-scale radiological events, a logical approach is complete automation of standard biodosimetric assays that are currently performed manually. The authors describe progress to date on the RABIT (Rapid Automated BIodosimetry Tool), designed to score micronuclei or γ-H2AX fluorescence in lymphocytes derived from a single drop of blood from a fingerstick. The RABIT system is designed to be completely automated, from the input of the capillary blood sample into the machine to the output of a dose estimate. Improvements in throughput are achieved through use of a single drop of blood, optimization of the biological protocols for in situ analysis in multi-well plates, implementation of robotic-plate and liquid handling, and new developments in high-speed imaging. Automating well-established bioassays represents a promising approach to high-throughput radiation biodosimetry, both because high throughputs can be achieved, but also because the time to deployment is potentially much shorter than for a new biological assay. Here the authors describe the development of each of the individual modules of the RABIT system and show preliminary data from key modules. System integration is ongoing, followed by calibration and validation.

INTRODUCTION

THE DEVELOPMENT of improved methods for radiation biodosimetry has been identified as a high-priority need in an environment of heightened concern over possible radiological or nuclear terrorist attacks (Pellmar and

* Center for Radiological Research, Columbia University Medical Center, New York, NY 10032; [†] Department of Mechanical Engineering, Columbia University, New York, NY 10027; [‡] Current address: Canadian Space Agency, Saint-Hubert, Quebec J3Y 8Y9, Canada.
For correspondence contact: Sally A. Amundson, Center for Radiological Research, Columbia University Medical Center, 630 West 168th Street, New York, NY 10032, or email at saa2108@columbia.edu.

Rockwell 2005). The detonation of even a small dirty bomb (radiological dispersal device) in a large metropolitan area would be likely to create large-scale panic, despite the low risk of radiological injuries. A small improvised nuclear device (IND) would produce a major health emergency in addition to mass panic. In such situations, in that the general population would not be carrying physical dosimeters, a very high throughput means of assessing the radiation exposure based on biological endpoints will be needed. This will serve both to reduce panic by reassuring those who were not significantly exposed, as well as triaging those in need of medical attention.

Cytogenetic assays have long been used in radiation biodosimetry and have been integrated into plans for response to radiological accidents (Lloyd et al. 1975; Huber et al. 1983; Fenech et al. 2003a; Wilkins et al. 2008; Blakely et al. 2009). While a variety of new biodosimetric assays are being developed (Blakely et al. 2001; Marchetti et al. 2006; Paul and Amundson 2008; Turtoi et al. 2008; Tyburski et al. 2008), there are considerable advantages to using more established mature assays, particularly in terms of time to deployment. Currently, established assays are generally manually performed, either in part or in whole, and thus are inadequate for high-throughput requirements. One approach to this problem is to use multiple laboratories, and this approach is being investigated (Wilkins et al. 2008; Blakely et al. 2009), though the logistics of such an approach may prove formidable in the context of a large-scale radiological event. An alternate approach is to speed up assays that are currently performed manually through automation; in fact, some components of these assays have been automated to a greater or lesser extent. For example, there has been considerable attention paid to automation of cytogenetic image analysis (Graham and Taylor 1980; Castleman et al. 1997; Odawara et al. 1997; Schunck et al. 2004; Decordier et al. 2009), and

various other components of biodosimetric assays have also been automated (Hayata et al. 1992; Martin et al. 2007). In practice, however, a very high-throughput system would require that the entire assay be fully automated, with no human intervention from start to finish.

The RABIT represents these authors' approach to achieving this complete automation. The authors describe here the overall design of the RABIT, details of the development of its individual modules in the context of these high-throughput goals, and describe preliminary data from key individual modules.

A FULLY AUTOMATED HIGH-THROUGHPUT RADIATION BIODOSIMETRY SYSTEM

The Rapid Automated BIodosimetry Tool (RABIT) is designed to be a completely automated, ultra-high throughput, robotically-based biodosimetry workstation (Salerno et al. 2007). It analyzes fingerstick-derived blood samples (30 μL, essentially a single drop of blood), either to estimate past radiation dose or to identify individuals exposed above or below a cutoff dose.

The RABIT automates two mature, but currently manual, biodosimetry assays [micronucleus (IAEA 2001; Fenech et al. 2003b) and γ-H2AX (Nakamura et al. 2006)], both of which have been shown to be highly radiation specific at the radiation doses of interest here. The use of mature assays is important for timely deployment, not least because FDA requirements are generally less burdensome than for a new bio-assay.

Based on measurements with these biomarkers, the RABIT is designed to estimate whole-body doses of 0.75 to 8 Gy, with a 95% confidence interval of ±20% at 1 Gy. A higher-throughput option for identifying individuals below/above a cutoff dose can potentially be applied. The RABIT is designed initially to have a throughput of ~6,000 samples per day, with parallelizing various steps potentially increasing this to 30,000 samples per day. Improved precision, if required, can be balanced against reduced throughput. There are a number of potential obstacles to achieving these target throughputs, and the RABIT addresses these by incorporating the following key technological innovations:

- Use of small volumes of blood (~30 μL) from a lancet fingerstick; this is a minimally invasive, and thus high throughput, approach to sample acquisition— conventional venipuncture-based blood collection is not compatible with ultra-high throughput;
- Complete robotically-based automation of the biology, with processing and imaging performed in situ in multi-well plates; this allows rapid processing of multiple simultaneous samples. The use of filter-bottomed multi-well plates allows faster reagent changes and prevents loss of cells during processing; and
- Innovations in high-speed imaging allow rapid analysis following biological processing.

As discussed above, although individual parts of cytogenetically-based bioassays have previously been automated (Hayata et al. 1992; Schunck et al. 2004; Martin et al. 2007), the authors know of no other system designed for complete automation. This aspect, together with the use of fingerstick samples and high-speed imaging innovations, are the basis for the high throughput of the RABIT.

Bioassays used in the RABIT

The RABIT is based on full automation of two well-characterized biodosimetric assays: the micronucleus assay (IAEA 2001; Fenech et al. 2003b) and the γ-H2AX assay (Nakamura et al. 2006). Only one assay can be done at a time, and the changeover time between assays is approximately 1 hour. Both assays, as implemented manually, are in current use in radiation biodosimetry and are highly radiation-specific at the radiation doses of interest here (da Cruz et al. 1994; Fenech et al. 1997; Livingston et al. 1997; IAEA 2001; Rothkamm et al. 2007).

The γ-H2AX assay is a direct measure of the number of DNA double strand breaks (DSB) that are present. It measures DSB by immune-staining the phosphorylated H2AX histone, which localizes to them. γ-H2AX yields can be quantified either by counting foci or integrating the fluorescent intensity (see Fig. 1a). The yield of γ-H2AX foci has been shown to be linearly related to dose over a very wide dose range (Rothkamm and Lobrich 2003). This assay gives a same-day result but requires that the blood samples are available within about 36 h of irradiation.

The micronucleus assay quantifies radiation-induced chromosome damage expressed as post-mitotic micronuclei, and there is a monotonic relationship between radiation-induced micronuclei yield and dose. Lymphocytes are cultured to division, but cytokinesis is blocked, preventing separation of the two daughter cells; healthy lymphocytes form binucleate cells, while those with chromosome damage can additionally contain one or more micronuclei containing chromosomal fragments (Fig. 1b). An important advantage of the micronucleus assay is that the signal is comparatively stable for some months post-exposure with a biological half life of about 12 mo (IAEA 2001; Thierens et al. 2005), so the need for early acquisition of blood samples is removed. While the relationship between micronucleus yield and doses is slightly non-linear over the dose range of interest
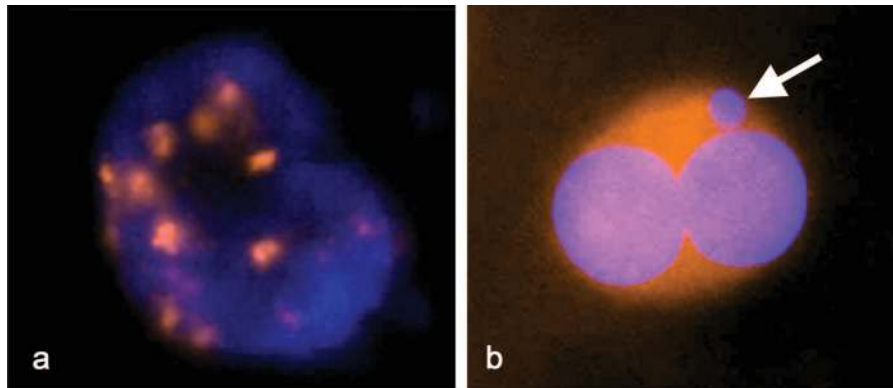
Fig. 1. Irradiated lymphocytes on RABIT filter membranes: (a) the γ-H2AX assay: Here the large blue blob corresponds to the nucleus, and the orange foci correspond to DNA double-strand breaks; the total amount of green fluorescence is the measured quantity; (b) the micronucleus assay: Here the orange blob is the cytoplasm, the two large blue blobs are divided binucleates, and the small blue blob is a micronucleus.

(Prosser et al. 1988; Műller and Rode 2002), the micronucleus yield does increase monotonically with doses up to 8 Gy (actually up to ~10 Gy), so the non-linearity can be simply accounted for with an appropriate calibration curve. Due to the required culture time, analysis time for this assay is approximately 70 h.

Both assays have comparatively low background values which are slightly age-dependent (Peace and Succop 1999; Sedelnikova et al. 2008). This limits their utility in a high-throughput mode at very low doses (e.g., ≤0.75 Gy); however, the RABIT is primarily designed for assessing higher doses (>0.75 Gy) to guide medical triage.

Due to the short lifetime of γ-H2AX foci, only samples arriving at the RABIT within 36 h of the event will be analyzed using the γ-H2AX assay. At 36 h post-event the RABIT will be re-configured, and all subsequent samples will be analyzed using the micronucleus assay. This approach allows all samples to be analyzed using the faster γ-H2AX assay during the 36-h time window when this assay can be used.

RABIT system overview

The RABIT is designed as a completely automated robotically-based system. After the fingerstick blood samples are input into the system, the samples are centrifuged through automated robotics to separate the lymphocytes, and preliminary lymphocyte quantification indicates if emergency treatment is required. The capillary is then laser-cut below the lymphocyte band and the lymphocytes deposited into filter-bottomed multi-well plates, one well per sample. The use of filter-bottomed plates allows rapid washes without the need to pellet and re-suspend after each step, simplifying the liquid-handling system and increasing throughput. Following

lymphocyte culturing (for the micronucleus assay), fixation and staining, the filter bottoms containing the samples are removed from the multi-well plates and sealed prior to automated high-speed imaging. Analysis of the images is performed online using dedicated image processing hardware to generate the dosimetric estimates. Finally, both the sealed filters and the images are archived.

The RABIT system consists of several linked modules: sample collection, lymphocyte separation, liquid handling and (for micronucleus) incubation, imaging, and data storage (Salerno et al. 2007). A service robot (RS80 SCARA, Staubli Robotics, Duncan, SC) transports samples between the various modules. The layout of the RABIT and a photo of the current breadboard prototype are shown in Fig. 2. Progress in the development of each of the RABIT modules is described in the following.

Development of sample collection module

The system is designed to process blood samples collected into barcoded plastic capillary tubes at the collection site(s) using a standard minimally-invasive fingerstick (lancet). Use of very small samples (30 μL) obtained through a fingerstick is one of the key aspects that enables high-throughput sample collection in the field. Conventional blood-sample acquisition through venipuncture is not compatible with ultra-high throughput.

The authors anticipate multiple fingerstick collection sites following a radiological event, such as doctors' offices, church halls, PoD (Point of Dispensing) sites, hospitals, etc. At these locations, field collection kits, consisting of lancets, barcoded capillary tubes (Fig. 3a) with matched personal data cards, alcohol wipes, and
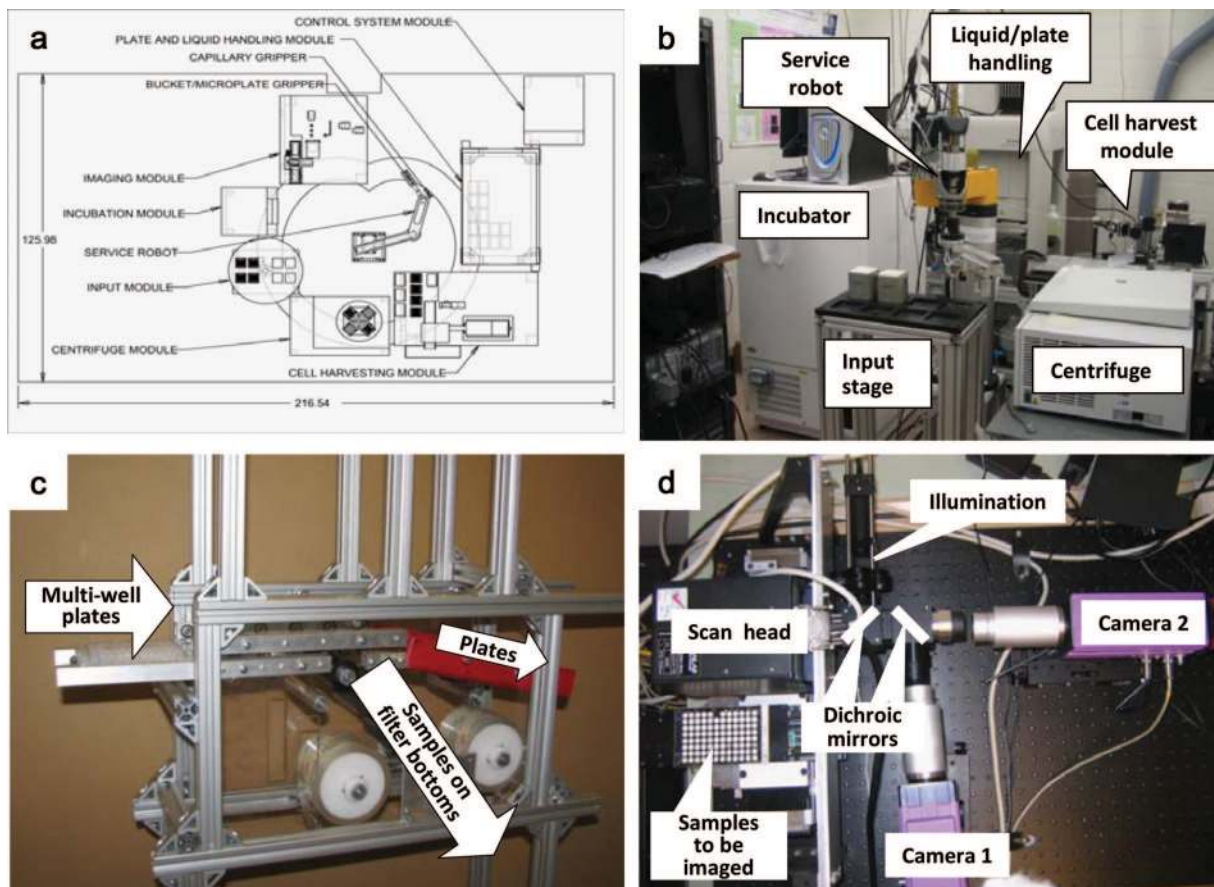
Fig. 2. (a) Schematic of RABIT layout; (b) breadboard prototype; (c) prototype transfer-to-substrate system; (d) prototype imaging system.
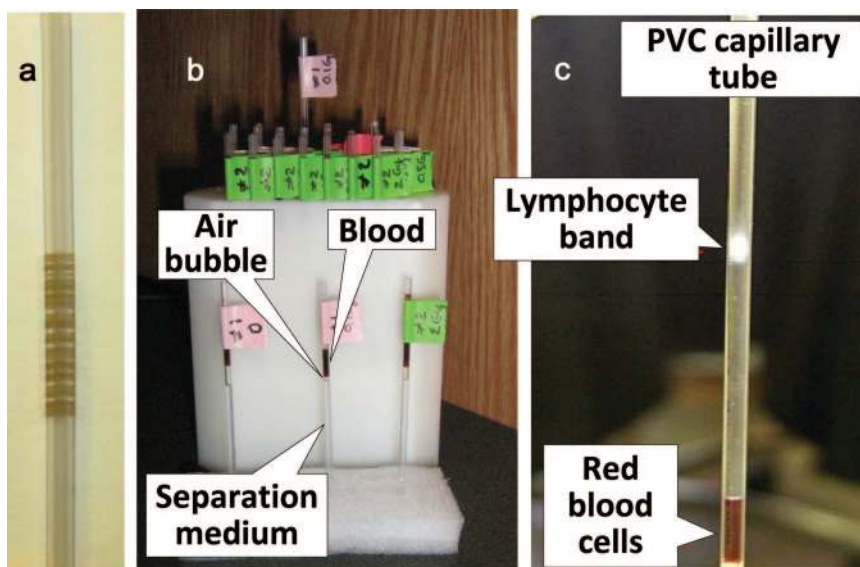

Fig. 3. (a) A barcoded capillary from the RABIT system. (b) A 32-capillary holder from the RABIT, loaded with blood-filled capillaries in Arizona and then shipped to New York. As seen in three capillaries shown outside the holder, a good layering of blood and separation medium was seen after this transport exercise. (c) A capillary after automated centrifuging, showing good separation between the lymphocyte band and the red blood cells.

sample holders for 32 filled capillaries (Fig. 3b) will be used to collect the samples.

To refine the requirements for the collection kit, a variety of lancets were tested with a wide range of blade sizes and penetration depths to optimize blood flow with minimal pain. Microtainer Contact-Activated Genie Lancets (BD Diagnostics, Franklin Lakes, NJ) have proven reliable in providing a 50-μL blood sample, more than the required volume.

Blood is drawn into heparin-coated PVC Safe-T-Fill capillaries (RAM Scientific, Yonkers, NY), which have been barcoded by laser etching. The blood-filled capillaries are then loaded into centrifuge inserts that are prefilled with Hemato-Seal Capillary Tube Sealant (Fisher Scientific, Pittsburgh, PA) and separation medium (Histopaque-1083, Sigma Aldrich, St. Louis, MO). As the blood in the capillary does not reach its edge, an air bubble is trapped between the blood and separation medium, preventing their mixing during transportation. This allows the sample to be collected by an individual with minimal training while maintaining the required layering of the blood and separation medium.

Fig. 3b shows sample capillaries which, in a transport exercise, were loaded with sealant, separation medium, and blood in Arizona and then shipped to New York using a commercial carrier. No spillage occurred in any of the 32 samples, and the lymphocytes were viable on arrival at the RABIT.

Development of the lymphocyte separation module

The lymphocyte separation module is designed to separate the lymphocytes in the blood sample through centrifugation, and then to dispense them into filter bottomed multi-well plates.

After transport to the RABIT, each holder containing 32 capillaries is loaded manually into centrifuge buckets on the input stage, after which there is no further human intervention. The buckets are then loaded by a service robot into an automated centrifuge. An interface board, lid opener, and a brake have been incorporated into an Eppendorf 5810R centrifuge (Eppendorf Corporation, Westbury, NY), allowing full robotic control.

Standard lymphocyte separation protocols have been modified to reproducibly separate lymphocytes from 30 μL of whole blood loaded on 50 μL of separation medium (Histopaque-1083, Sigma Aldrich, St. Louis, MO). Optimum separation is achieved when samples are spun at 4,000 rpm for 5 min. Using this protocol, lymphocytes separated from whole blood form a compact cloud of essentially 100% purity (i.e., no red blood cell contamination), typically containing ~3,000 lymphocytes/μL (Fig. 3c).

Following centrifugation, the service robot removes centrifuge buckets from the centrifuge using a pneumatic

bucket gripper, after which a capillary gripper services individual capillaries. Each capillary is first brought into the field of view of the barcode reader for identification. Since the barcode etched on the capillary is necessarily very small (Fig. 3a), barcode reading reliability is an issue: The current successful reading rate, based on a triple read, is 95%. The remaining error is due to rotational misalignment of the capillary barcode, and will be addressed by rotating the capillary so that its barcode faces the reader.

The capillary is then moved into the field of view of a CCD camera and imaged (Fig. 3c). The boundary between culture medium and red blood cells is located using custom image analysis software, the lymphocyte band being located ~40 mm above this boundary, corresponding to 50 μL of separation medium. During this imaging stage, a rough estimate of the lymphocyte count is obtained by quantitative imaging of the lymphocyte band; this allows flagging of individuals with acute lymphocyte depletion.

The capillary is moved vertically such that an Osprey UV laser (Quantronix Lasers, East Setauket, NY) cuts the capillary 9 mm above the boundary (i.e., ~30 mm below the lymphocyte band). During cutting, the capillary is rotated by the gripper motor to improve the cutting speed and reduce the required laser power.

Finally, the pellet containing red blood cells is ejected, and the cut capillary containing lymphocytes and plasma is moved above the appropriate well of the microplate. Once the capillary reaches the correct position, pressurized air is introduced to the top of the capillary, emptying the lymphocytes into the well. The measured timings of the various steps are shown in Table 1.

Development of the liquid handling and (for micronucleus) incubation module

The liquid-handling system can be configured to perform either the micronucleus or the γ-H2AX assay,

Table 1. Processing time for lymphocyte harvesting, based on measurements using the current breadboard prototype RABIT. The total time corresponds to a throughput of 6,500 samples per 20 hour day.

Step	Time (sec)	
	Total	Per sample
Load four buckets into centrifuge	97.5	0.25
Centrifugation	370.0	0.96
Unload centrifuge	52.8	0.14
Transfer one multi-well plate from stack to dispense position	6.8	0.07
Pick up one capillary, image and locate lymphocyte band, cut capillary, read barcode, dispense lymphocytes, dispose of tube	9.64	9.64
Total		11.06

with a rapid switchover between the assays. All processing is performed in situ in filter-bottomed multi-well plates. This allows for easy replacement of reagents in the wells: The reagents are drained through the filter bottoms and then new reagents are added. The filter pore size is chosen so that the lymphocytes are not lost at this stage. This approach eliminates the need for centrifugation and re-suspension of the cells at each addition of reagents and the loss of lymphocytes at each step. The liquid-handling system is coupled to a robotic incubator, which is required for culturing cells in the micronucleus assay.

The standard protocols are optimized for the two assays in terms of reagent concentrations and quantities, incubation times, etc., for use in 96-well plates with a robotic-based system. The modified protocols are summarized in Fig. 4.

The fully automated liquid/plate-handling module is a commercial system, Sciclone ALH3000 (Caliper Life Sciences, Hopkinton, MA). The ALH3000 workstation is a flexible, automated liquid-handling workstation that can be configured to handle cell-based assays. The ALH3000 deck has 18 positions that are used for several reagent reservoirs, multi-well plates, a waste disposal station, and an ultrasonic bath (for cleaning the liquid dispensers). It also has a gantry system that can carry either a 96-cannula array for dispensing reagents, or a positive pressure unit that is used for purging liquid from the wells into the waste system. The gantry also has a gripper for moving multi-well plates, and an 8-channel bulk dispenser for dispensing larger quantities of reagents (e.g., for filling wells with cell culture medium).

Using the manufacturer-supplied software, the ALH3000 workstation has been programmed to perform the micronucleus or γ-H2AX assays summarized in Fig. 5. The ALH300 workstation communicates with the service robot via a 4-bit digital interface. If the plate needs to be incubated (i.e., for the micronucleus assay), it is placed on the "unload" position on the deck and a

signal sent to the service robot, which transfers it to a Liconic STX220 robotic incubator (Liconic US Inc., Woburn, MA).

Development of the high-speed automated imaging module

After the biological processing is complete, the multi-well plates are moved within the RABIT to the integrated imaging system (Fig. 2d), where the fixed, stained lymphocytes are imaged on the filter membranes that comprise the bottom of each well.

Prior to the imaging procedures, in order to accommodate the short working distance of the imaging optics, as well as to generate compact, sealed archival specimens, the filter bottoms are detached from each multi-well plate, transferred to an adhesive surface and sealed using a transparent adhesive film to keep them intact. To accomplish this, an automated system for transferring the filter bottoms onto a continuous roll of film has been developed (Fig. 2c). As the plate is moved through this system, a pneumatic gripper removes the underdrain, providing access to the filters. Adhesive film is then pressed on the filters and gently pulled off, carrying with it the attached filter bottoms which are then sealed using a second layer of the same film. The authors have tested several commercially-available adhesive and lamination films for clarity and low autofluorescence. Clear View packing tape (Staples Inc., Framingham, MA) or acetate plate sealing tape (Corning Inc., Lowell, MA) were found to be optimal. Once the filter bottoms are attached and sealed, the continuous film containing the filter bottoms is fed into the imaging system and, after imaging, collected on a roll for archiving.

Despite much current focus on high-throughput imaging systems (Gough and Johnston 2007), in fact no commercial system is fast enough with adequate spatial resolution to allow the targeted throughput. The RABIT imaging system incorporates three novel techniques, briefly described here, for speeding up imaging: use of
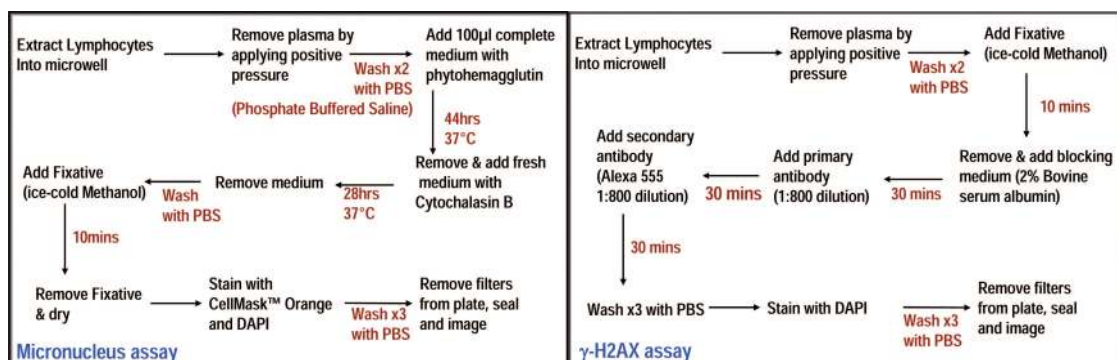

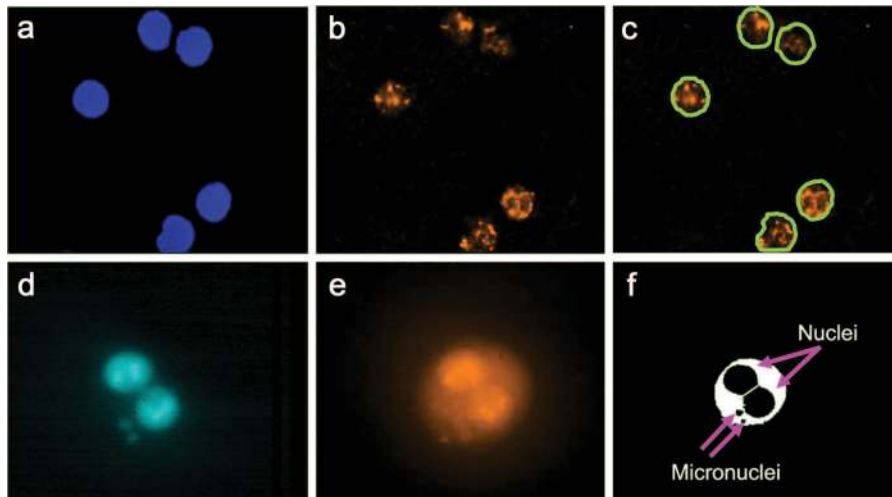**Fig. 4.** Current RABIT protocols for the micronucleus assay (left) and the γ-H2AX assay (right).

Fig. 5. RABIT image analysis. Top: γ-H2AX analysis: (a) imaged nuclei; (b) imaged γ-H2AX fluorescence; (c) γ-H2AX fluorescence integrated within the boundaries of each nucleus (green line). Bottom: Micronuclei analysis: (d) imaged nuclei; (e) imaged cytoplasm; (f) nucleus and cytoplasm images are binarized, subtracted, and "holes" scored.

light steering rather than sample motion, single-step auto-focusing, and parallel use of multiple high-speed CMOS cameras. Using these techniques, an imaging time of significantly less than 10 s per sample has been achieved:

- Light steering: In order to obtain sufficient statistics, about one hundred 200-μm frames (fields of view) need to be imaged for each sample. Typically, imaging different frames within the same sample is achieved by mechanically moving a stage carrying the samples. However, mechanical motion takes tens of milliseconds per motion, which is too slow. Instead of moving the sample, in the RABIT the light is steered into the camera using fast galvanometric mirrors (HurryScan II, ScanLab America Inc., Saint Charles, IL). Typical transit times between adjacent fields of view are less than 1 ms;

- One-step focusing is performed by incorporating an astigmatic element (a cylindrical lens) into one component of the optics. This results in a known focus-dependent distortion. For example, a spherical bead is imaged as an ellipse, and the aspect ratio of the ellipse indicates exactly how far the sample is out of focus. Based on this information from a single image, the objective, mounted on a piezolelectric actuator (Mad City Labs, Madison, WI), can be moved, allowing one-step (rather than iterative) focusing;

- Simultaneous use of multiple CMOS cameras, sensitive to the colors of different dyes, allows simultaneous acquisition of separate images of the cytoplasm (stained using Cell Mask Orange) and either the nucleus (stained using DAPI) or γ-H2AX foci (stained with Alexa fluor 555), as well as focus information.

The RABIT uses three CMOS Photonfocus MV-1024D-160E cameras (PhotonFocus, Lachen, Switzerland), which allow a continuous frame-rate of 150 frames per second. Each camera is mounted on a VS-1485 image intensifier (Videoscope International, Dulles, VA); and

- High-speed image analysis. Depending on which assay is being performed, different image analyses are carried out. Both assays can be simplified to the detection of "blobs and holes" rather than more complex morphometric structures, and thus the image analysis stages are very rapid, with a significant proportion of the analysis being done either in the CMOS cameras themselves or on the frame grabber card (Helios, Matrox Imaging, Dorval, QC) before being sent to the RABIT computer workstation. The analysis software is written in C++ using the Matrox imaging library, which allows for hardware acceleration of the analysis.

The sensitivity of the RABIT depends largely on the number of cells analyzed. For the micronucleus assay operating in "rapid triage" mode, the authors will analyze 250 binucleated cells per individual to obtain a dose precision of better than ±20% at 1 Gy; a smaller number of analyzed cells is required for the γ-H2AX assay (Rothkamm et al. 2007). The RABIT can be simply reprogrammed to analyze more cells per individual in order to obtain a more precise dose estimate at a cost of longer processing times.

Image analysis for the γ-H2AX assay is illustrated in Fig. 5a–c. Rather than count individual γ-H2AX foci, an equally accurate but faster approach is to measure the total γ-H2AX fluorescence within each cell. The DAPI fluorescent stain image is filtered, binarized, and the

boundaries of each cell nucleus identified (Fig. 5a). For each nucleus, the integrated fluorescent intensity (Fig. 5b) within each nuclear boundary (Fig. 5c) is scored. The average intensity over all counted cells is then compared to a calibration curve, and a dose estimate is generated. In the case of the γ-H2AX assay, time (post exposure)-dependent calibration curves will be generated and used to account for the decay of the γ-H2AX signal.

Image analysis for the cytokinesis-blocked micronucleus assay is illustrated in Fig. 5d–f. The raw images (Fig. 5d and e) are filtered and binarized, and a watershed algorithm is applied to separate touching objects. Then the two binary images (of nuclei and cytoplasms) are analyzed together: The binarized image of each nucleus is subtracted from the binarized image of the corresponding cytoplasm (Fig. 5f), and the nucleus belonging to each cell is identified in the subtracted image. Finally, the RABIT software scores the number of micronuclei (Fig. 5f: small holes) in binucleated cells (Fig. 5f: two large holes). The number of micronuclei scored for 250 binucleate cells is compared to a calibration curve, and a dose estimate is recorded.

Data archiving

Both the sealed substrate rolls containing the samples and the digital image data will both be archived for potential subsequent reconfirmation or for subsequent higher-precision reanalysis. The digital data (at full capacity, 17 TB per 20 h RABIT-d) is initially stored on high-capacity drives and moved daily to tape for long-term storage.

CONCLUSION

The authors describe here progress toward a completely automated high-throughput approach to radiation biodosimetry following a large-scale radiological event. The approach uses robotically-based in situ biological processing in multi-well plates, as well as novel imaging techniques, to facilitate high-throughput screening of small fingerstick-derived blood samples. The two comparatively mature assays used, micronucleus and γ-H2AX, are well established, sensitive over a wide range of relevant doses, and can potentially be used for partial-body as well as total-body exposures (Senthamizhchelvan et al. 2008). The authors believe that automating well-established bioassays represents a promising approach to high-throughput radiation biodosimetry, both because high throughputs can be achieved, but also because the time to deployment is potentially much shorter than for a new biological assay. At present, all the individual modules of the RABIT system, which have been described here, are functional and performing to specification. Integration of the modules, followed by calibration and validation, are ongoing.

REFERENCES

Blakely WF, Carr Z, Chu MC, Dayal-Drager R, Fujimoto K, Hopmeir M, Kulka U, Lillis-Hearne P, Livingston G, Lloyd DC, Maznyk N, Perez Mdel R, Romm H, Takashima Y, Voisin P, Wilkins RC, Yoshida MA. WHO 1st consultation on the development of a Global Biodosimetry Laboratories Network for radiation emergencies (BioDoseNet). Radiat Res 171:127–139; 2009.

Blakely WF, Prasanna PGS, Grace MB, Miller AC. Radiation exposure assessment using cytological and molecular biomarkers. Radiat Protect Dosim 97:17–23; 2001.

Castleman KR, Schulze M, Wu Q. Automated biodosimetry using digital image analysis of fluorescence in situ hybridization specimens. Radiat Res 148:S71–S75; 1997.

da Cruz AD, McArthur AG, Silva CC, Curado MP, Glickman BW. Human micronucleus counts are correlated with age, smoking, and cesium-137 dose in the Goiânia (Brazil) radiological accident. Mutat Res 313:57–68; 1994.

Decordier I, Papine A, Plas G, Roesems S, Vande Loock K, Moreno-Palomo J, Cemeli E, Anderson D, Fucic A, Marcos R, Soussaline F, Kirsch-Volders M. Automated image analysis of cytokinesis-blocked micronuclei: an adapted protocol and a validated scoring procedure for biomonitoring. Mutagenesis 24:85–93; 2009.

Fenech M, Bonassi S, Turner J, Lando C, Ceppi M, Chang WP, Holland N, Kirsch-Volders M, Zeiger E, Bigatti MP, Bolognesi C, Cao J, De Luca G, Di Giorgio M, Ferguson LR, Fucic A, Lima OG, Hadjidekova VV, Hrelia P, Jaworska A, Joksic G, Krishnaja AP, Lee TK, Martelli A, McKay MJ, Migliore L, Mirkova E, Műller WU, Odagiri Y, Orsiere T, Scarfi MR, Silva MJ, Sofuni T, Surralles J, Trenta G, Vorobtsova I, Vral A, Zijno A. Intra- and inter-laboratory variation in the scoring of micronuclei and nucleoplasmic bridges in binucleated human lymphocytes. Results of an international slide-scoring exercise by the HUMN project. Mutat Res 534:45–64; 2003a.

Fenech M, Chang WP, Kirsch-Volders M, Holland N, Bonassi S, Zeiger E. HUMN project: detailed description of the scoring criteria for the cytokinesis-block micronucleus assay using isolated human lymphocyte cultures. Mutat Res 534:65–75; 2003b.

Fenech M, Perepetskaya G, Mikhalevich L. A more comprehensive application of the micronucleus technique for biomonitoring of genetic damage rates in human populations—experiences from the Chernobyl catastrophe. Environ Mol Mutagen 30:112–118; 1997.

Gough AH, Johnston PA. Requirements, features, and performance of high content screening platforms. Methods Molec Biol 356:41–61; 2007.

Graham J, Taylor CJ. Automated chromosome analysis using the Magiscan image analyzer. Anal Quant Cytol 2:237–242; 1980.

Hayata I, Tabuchi H, Furukawa A, Okabe N, Yamamoto M, Sato K. Robot system for preparing lymphocyte chromosome. J Radiat Res 33:231–241; 1992.

Huber R, Streng S, Bauchinger M. The suitability of the human lymphocyte micronucleus assay system for biological dosimetry. Mutat Res 111:185–193; 1983.

IAEA. Cytogenetic analysis for radiation dose assessment: a manual. Vienna: International Atomic Energy Agency; 2001.

Livingston GK, Jensen RH, Silberstein EB, Hinnefeld JD, Pratt G, Bigbee WL, Langlois RG, Grant SG, Shukla R. Radiobiological evaluation of immigrants from the vicinity of Chernobyl. Int J Radiat Biol 72:703–713; 1997.

Lloyd DC, Purrott RJ, Dolphin GW, Bolton D, Edwards AA, Corp MJ. The relationship between chromosome aberrations and low LET radiation dose to human lymphocytes. Int J Radiat Biol Relat Stud Phys Chem Med 28:75–90; 1975.

Marchetti F, Coleman MA, Jones IM, Wyrobek AJ. Candidate protein biosimeters of human exposure to ionizing radiation. Int J Radiat Biol 82:605–639; 2006.

Martin PR, Berdychevski RE, Subramanian U, Blakely WF, Prasanna PGS. Sample tracking in an automated cytogenetic biodosimetry laboratory for radiation mass casualties. Radiat Meas 42:1119–1124; 2007.

Műller WU, Rode A. The micronucleus assay in human lymphocytes after high radiation doses (5–15 Gy). Mutat Res 502:47–51; 2002.

Nakamura A, Sedelnikova OA, Redon C, Pilch DR, Sinogeeva NI, Shroff R, Lichten M, Bonner WM. Techniques for gamma-H2AX detection. Methods Enzymol 409:236-250; 2006.

Odawara K, Yamamoto K, Kato H, Hara M, Kogiso S, Kishida F, Yoshitake A, Nakatsuka I. A new semi-automated chromosome analysis system for in vitro chromosomal aberration tests. Mutat Res 389:207–212; 1997.

Paul S, Amundson SA. Development of gene expression signatures for practical radiation biodosimetry. Int J Radiat Oncol 71:1236–1244; 2008.

Peace BE, Succop P. Spontaneous micronucleus frequency and age: what are normal values? Mutat Res 425:225–230; 1999.

Pellmar TC, Rockwell S. Priority list of research areas for radiological nuclear threat countermeasures. Radiat Res 163:115–123; 2005.

Prosser JS, Moquet JE, Lloyd DC, Edwards AA. Radiation induction of micronuclei in human-lymphocytes. Mutat Res 199:37–45; 1988.

Rothkamm K, Balroop S, Shekhdar J, Fernie P, Goh V. Leukocyte DNA damage after multi-detector row CT: a quantitative biomarker of low-level radiation exposure. Radiol 242:244–251; 2007.

Rothkamm K, Löbrich M. Evidence for a lack of DNA double-strand break repair in human cells exposed to very low x-ray doses. Proc Natl Acad Sci USA 100:5057–5062; 2003.

Salerno A, Zhang J, Bhatla A, Lyulko OV, Dutta A, Garty G, Simaan N, Pehrson GR, Yao YL, Brenner DJ, Nie J. Design considerations for a minimally invasive high-throughput automation system for radiation biodosimetry. In: IEEE International Conference on Automation Science and Engineering, 2007 CASE 2007. Piscataway, NJ: IEEE; 2007: 846–852.

Schunck C, Johannes T, Varga D, Lörch T, Plesch A. New developments in automated cytogenetic imaging: unattended scoring of dicentric chromosomes, micronuclei, single cell gel electrophoresis, and fluorescence signals. Cytogenet Genome Res 104:383–389; 2004.

Sedelnikova OA, Horikawa I, Redon C, Nakamura A, Zimonjic DB, Popescu NC, Bonner WM. Delayed kinetics of DNA double-strand break processing in normal and pathological aging. Aging Cell 7:89–100; 2008.

Senthamizhchelvan S, Pant GS, Rath GK, Julka PK, Nair O, Prabhakar R, Malhotra A. Biological estimation of dose in hemi-body irradiation of cancer patients by cytogenetic analysis. Health Phys 94:112–117; 2008.

Thierens H, De Ruyck K, Vral A, de Gelder V, Whitehouse CA, Tawn EJ, Boesman I. Cytogenetic biodosimetry of an accidental exposure of a radiological worker using multiple assays. Radiat Protect Dosim 113:408–414; 2005.

Turtoi A, Brown I, Oskamp D, Schneeweiss FHA. Early gene expression in human lymphocytes after gamma-irradiation—a genetic pattern with potential for biodosimetry. Int J Radiat Biol 84:375–387; 2008.

Tyburski JB, Patterson AD, Krausz KW, Slavik J, Fornace AJ, Gonzalez FJ, Idle JR. Radiation metabolomics. 1. Identification of minimally invasive urine biomarkers for gamma-radiation exposure in mice. Radiat Res 170:1–14; 2008.

Wilkins RC, Romm H, Kao TC, Awa AA, Yoshida MA, Livingston GK, Jenkins MS, Oestreicher U, Pellmar TC, Prasanna PGS. Interlaboratory comparison of the dicentric chromosome assay for radiation biodosimetry in mass casualty events. Radiat Res 169:551–560; 2008.

■ ■